Developments in the Effective Use and Interpretation of Lithogeochemistry in Regional Exploration Programs: Application of GIS Technology

Harris, J.R.[1], Grunsky, E.C.[2], Wilkinson, L.[3]

1. Geological Survey of Canada, Ottawa, Ontario, Canada
2. RGI, Vancouver, British Columbia, Canada
3. Geological Survey of Canada, Ottawa, Ontario, Canada

ABSTRACT

Geographic Information Systems (GIS) are being used with increasing frequency by the Canadian mineral exploration community as they are extremely useful for archiving and analysing a wide range of digital geoscience data. This paper summarizes GIS methods for compiling, evaluating, manipulating and visualizing a large lithogeochemical database over the Swayze Greenstone Belt, Ontario. The database has been assembled from diverse sources including both proprietary and non-proprietary, government databases. The data have been screened for inaccuracies and partitioned into altered and unaltered samples using a variety of methods. MgO major element oxide data are used to illustrate GIS processing and visualization methodologies, including ternary and 3-D scatterplots and map comparison methods.

INTRODUCTION

The objective of this paper is to discuss how lithogeochemical data can be analyzed with respect to regional mineral exploration using a Geographic Information System (GIS). Several diverse lithogeochemical datasets have been assembled for the Swayze Greenstone Belt in Northern Ontario (Figure 1) by industry and governments (provincial and federal) to assist on-going mapping and regional exploration (Harris *et al.*, 1994). The methodologies set forth in this paper can be used to assist geologists in compiling, evaluating and manipulating their own geochemical datasets with the aid of a GIS. This paper uses examples taken from Harris *et al.*, (1997) who provide more detailed accounts of the material summarized here.

Geographical Information Systems (GIS) are being used with increasing frequency in the Canadian mining industry. GIS are capable of storing, displaying and plotting georeferenced points, lines and polygon data. They also provide a wide range of spatial analysis tools with which to display, query, manipulate, visualize and analyse data. GIS have been used routinely for generating exploration favourability maps (Bonham-Carter *et al.*, 1988; Harris, 1989; Rencz *et al.*, 1994; Bonham-Carter, 1994; Harris *et al.*, 1995; Wright and Bonham-Carter, 1996).

The Swayze Greenstone Belt (SGB) is the westernmost extension of the mineral-rich Abitibi Greenstone Belt (AGB), and has recently been re-mapped by both the OGS and the GSC (Heather *et al.*, 1995; Ayer and Theriault, 1993). Similar to the AGB, the SGB contains a number of folded 2730-2680 Ma mafic-felsic metavolcanic packages that are unconformably overlain by Timiskaming-type metasedimentary rocks and cut by high strain zones thought to be extensions of the major "breaks" (Destor-Porcupine and Cadillac-Larder Lake Faults) found in the AGB. Unlike, the AGB however, few economic deposits have been found within the SGB. The relatively small size of the belt, the availability of large amounts of digital data, and lack of any major exploration efforts within the belt make the area ideal for study.

In a regional geochemical compilation program it is likely that data have been collected at different times, by different organizations using different sampling strategies and analysed by different laboratories using different analytical techniques. In order to make effective use and interpretation of combined lithogeochemical data for regional mapping and exploration activities the data must be scrutinized both statistically and spatially. Wilkinson *et al.*, (1997) provide details on the problems and solutions invoked in assembling this database.

DATA ANALYSIS

Central to the analysis procedure is the GIS, where all data are archived. However, certain assessment procedures necessitate use of additional software (e.g., statistical analysis packages) for access to functionality not available within the GIS. The import and export of data to the GIS is accomplished through the use of ASCII text files (and associated header files when required) or common database formats such as Lotus, d-Base and Microsoft Access.

In "Proceedings of Exploration 97: Fourth Decennial International Conference on Mineral Exploration" *edited by* A.G. Gubins, 1997, p. 285–292

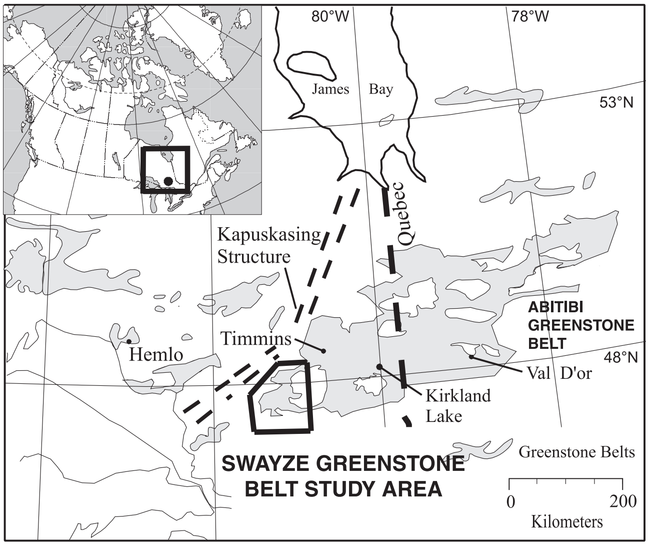

Figure 1: *General location of the Swayze Greenstone Belt in Ontario.*

Alteration

If the database is to be used to assist in lithologic characterization for exploration and mapping it is beneficial to separate altered from unaltered geochemical samples. Many methods exist for identifying altered samples (Rollinson, 1993, Madiesky and Stanley, 1993). In this study the following methods were used to flag altered samples:

1. excessive LOI (> 8% for mafic rocks and > 4% for felsic rocks),
2. excessive volatiles ($CO_2 + H_2O$) > 3.8%,
3. alteration index (H.I. > 49 and ACNK index > .72),
4. atypical minerals based on normative mineral classification,
5. index of typicality (or atypicality index) (Grunsky *et al.*, 1992) and,
6. identification of anomalous trends on 3-D scatterplots.

The thresholds for LOI were based on consultation with various exploration companies (Falconbridge in particular) and a number of government field geologists (Ayer, per comm.; OGS, 1996). Typically, regional metamorphosed mafic rocks have high LOI values due to greater abundance's of hydrous minerals (micas and amphiboles). Thresholds for total volatile content were set based on upper breakpoints observed on probability plots of the data (Figure 6). The alteration indices were chosen in consultation with Falconbridge Ltd. who have used them for base metal exploration in various greenstone belts throughout northern Ontario. The Hashimoto index (H.I.) is defined as follows:

$$((MgO + K_2O) / (MgO + K_2O + CaO + Na_2O)) \times 100 \qquad [1]$$

and the ACNK index is defined as:

$$Al_2O_3 / (NA_2O + CAO + K_2O) \qquad [2]$$

The H.I. index emphasizes MgO mobility over alkali depletion and thus is useful for detecting alteration in mafic and ultramafic rocks. The ACNK index is used for detecting Al_2O_3 mobility over alkali depletion and is useful for detecting the alteration of feldspars, and thus is more appropriate for intermediate to felsic rocks.

A normative mineral classification was undertaken using the major element oxide data. A function using S+ statistical software was written to perform the classification and the results were imported to GIS as an ASCII file. Altered samples were flagged based on atypical minerals using the following criteria: hematite (or) wollastonite (or) pervoskite (or) nepheline (or) leucite (or) kaliophilite (or) calcium silicate (or) acmite (or) sodium silicate (or) potassium silicate > 0% and/or corrundum > 3%.

An alteration statistic based on the index of typicality was also used (Grunsky *et al.*, 1992). The index of typicality is a measure of how typical a sample is with respect to a reference population of samples (e.g., calc-alkaline basalts, ultramafic komatiites) established for Archean volcanic rocks within the Abitibi greenstone belt (Grunsky *et al.*, 1992). An index of typicality of 0.9 means a sample has a high probability of belonging to the specific reference population while an index of 0 indicates that the sample under consideration does not belong to the group and perhaps represents an altered sample.

Altered samples can also be identified on 3-D scatterplots of major element data. Figure 2 shows scatterplots of Fe_2O_3, Al_2O_3, CaO and MgO concentration for all volcanic samples within the northern portion of the greenstone belt. A brushing technique was employed to identify unusual data trends on these scatterplots (see samples in red on Figure 2). The spatial distribution of these samples can then be displayed on a geologic map (Figure 2). The unusual trend seen in the above scatterplots comprise 31 samples, 29 of which plot as ultramafic komatiites on a Jensen ternary diagram (Jensen, 1976). The remaining 2 samples fall within units mapped as mafic intrusions. All these samples have been flagged as altered, using the methods discussed above. This alteration trend, characterized by MgO mobility (enrichment), can be clearly seen on Figure 3 which is a Jensen ternary plot of altered versus unaltered samples for all mafic samples within the study area. This alteration trend will cause mafic samples to be misclassified as ultramafic samples. The challenge is to determine which samples may be associated with mineralization (see below).

Out of a total of 3396 "clean" samples, 1788 have been flagged as altered representing approximately 53% of the total. Table 1 shows the breakdown of altered samples by method. The thresholds based on the normative mineral classification and LOI are the most liberal having flagged 810 and 665 altered samples, respectively.

The GIS can be used to visualize the geochemical data in different ways. Figures 4a and 4b show bubble plots (proportional circles) of LOI and volatile abundance over the belt. Larger circles, reflecting greater abundance's, perhaps indicate alteration zones. Figures 4c and 4d are alternative visualization methods. These are RGB (red-green-blue) ternary maps showing alteration zones derived by combinations of the flagging methods. A maximum of 3 alteration maps can be combined in one image. The altered samples were converted to a raster grid by:

1. 1) converting each sample point to a raster cell (grid) using a point-to-grid conversion within the GIS,
2. calculate the average density of altered points for each grid cell using a 25 × 25 mean filter (~ 2.5 × 2.5 km filter size) and,
3. assign red, green and blue colours to the alteration grids (images).

In Figure 4d altered zones derived from atypical norm minerals, LOI and volatiles index have been displayed in red, green and blue colours, respectively. Spatial relationships between the alteration zones can be interpreted with reference to the mix of the additive primary colours, red, green and blue. For example, area B displayed in yellow indicates that this alteration zone is characterized by a relatively high percentage of atypical normative minerals (red) and high LOI values (green) as red plus green form a yellow colour. Areas in white are where all 3 methods used for flagging altered samples coincide. Table 2 is a summary of the major altered zones (locations A-G) identified on Figures 4c and 4d. All zones of intense alteration are located in high strain zones mapped by Heather *et al.* (1995) in the southern and central portions of the belt and in the northern area by Ayer and Theriault (1993). Zones C and B coincide with areas known to be mineralized (Shunsby zone and Old Women iron formation, respectively) while the other zones do not. Area A is particularly enigmatic and marks the intersection of two major shear zones (Ayer, oral comm.; Ontario Geological Survey).

Processing of Major Oxide Data for Mineral Exploration

The GIS can be used effectively to determine anomalous oxide element populations. The following example uses MgO as the greenstone belt comprises a high percentage of mafic and ultramafic volcanic rocks. However any other major or trace element may be analysed using this methodology (see Harris *et al.*, 1997).

Table 1: ***Altered samples flagged by alteration method.***

Alteration flag method	No. of samples	% of Total Samples[1]
Norm	810	23.8%
LOI	665	19.6%
Volatiles (Low)	260	7.6%
Volatiles (High)	89	2.6%
Index (Low)	432	12.7%
Index (High)	105	3.1%
Atypicality index	413	12.2%

1. Total samples is 3396.

Definition of Anomalies

Figure 5 show continuous surface maps of MgO concentration (weight percent) for the entire greenstone belt. The MgO map in Figure 5a has been interpolated from all the available geochemical samples

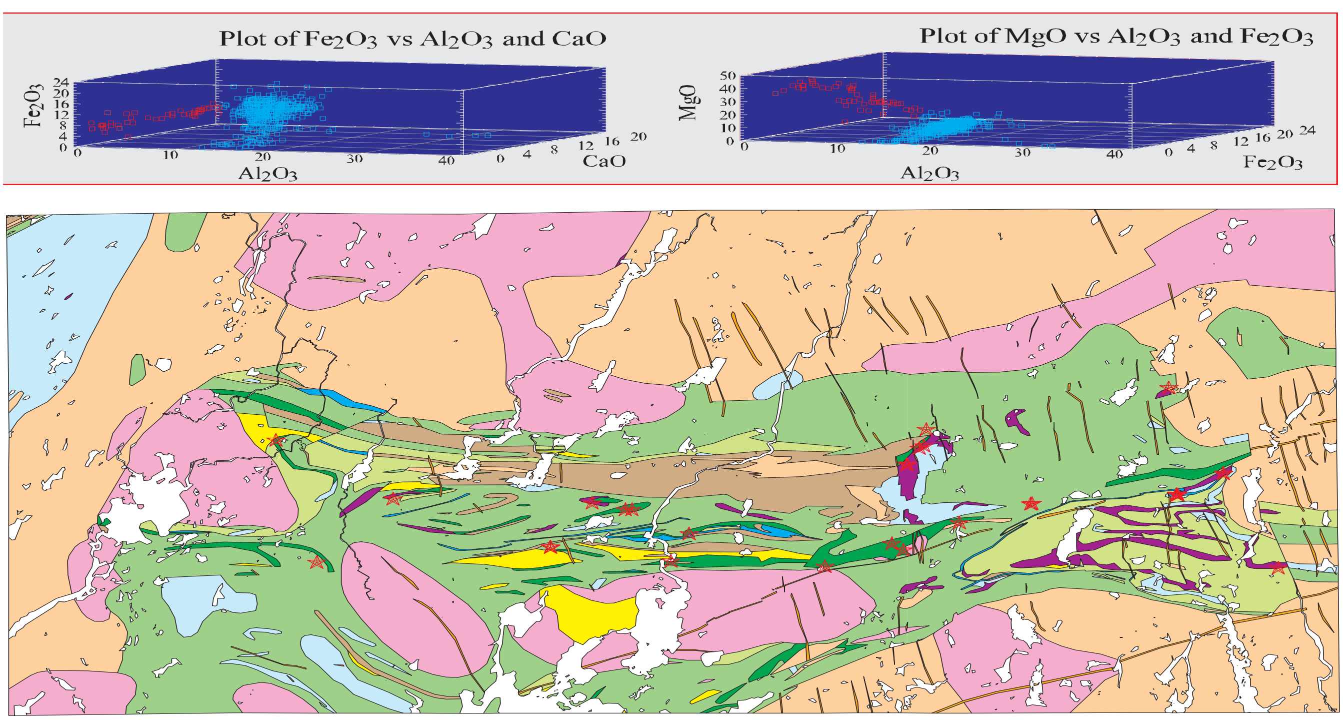

Figure 2: *Distribution of altered samples (red stars) in the northern portion of the Swayze greenstone belt. Altered samples were identified using 3-D scatterplot brushing of MgO, Al_2O_3 and Fe_2O_3 (see red samples in scatterplots above map).*

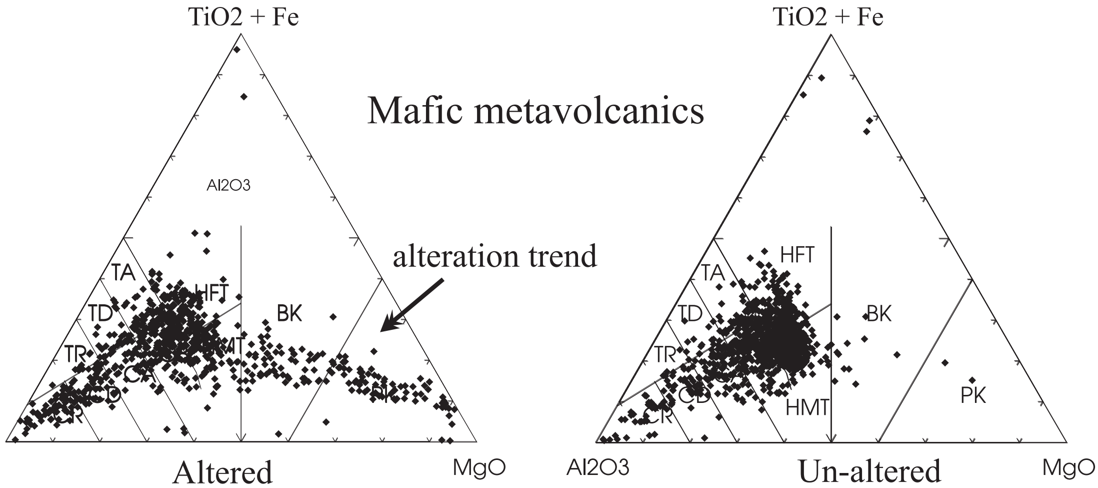

C = Calc-Alkaline, T = Tholeiitic , R = Rhyolites, D = dacites, B = basalts, A = andesites
HMT = high magnesium tholeiites, HFT = high iron tholeiites, BK = basaltic komatiites,
PK = ultramafic komatiites

Figure 3: *Jensen Ternary Plot of altered vs. un-altered samples for mafic volcanic lithologies.*

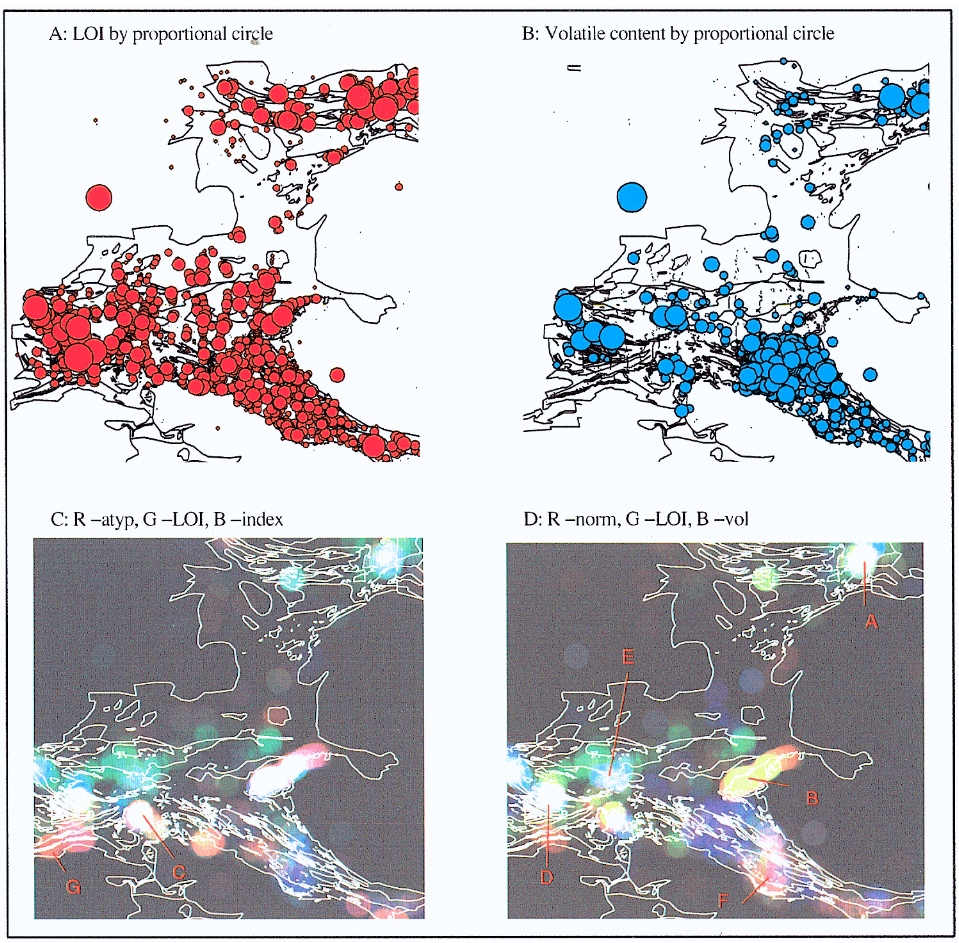

Figure 4: *Alternative methods of alteration visualization. Maps A and B show alteration via proportional circle plots of LOI and volatile content, respectively. Maps C and D show alteration in the form of RGB continuous surface ternary maps (R=red, G=green, B=blue).*

Table 2: ***Geological characteristics of altered zones (see Figure 4).***

Zone	Lithology	Alteration	Structure
A. Northeastern Swayze	mafic metavolcanics	LOI, volatiles, norm minerals, alteration index, atypicality index	intersection of two high strain zones as mapped by Ayer (1995)
B. Old Woman Fe Formation	oxide to sulphide facies iron formation	LOI, volatiles, norm minerals, alteration index, atypicality index	highly strained limb of large anticline
C. Shunsby Fe Formation	oxide to sulphide facies iron formation	LOI, volatiles, norm minerals, alteration index, atypicality index	
D. Western Swayze	mafic metavolcanics	LOI, volatiles, norm minerals, alteration index, atypicality index	high strain zone (continuation of Cadillac-Larder Lake "break")
E. Central Swayze	felsic metavolcanics	LOI, volatiles, alteration index	northern limb of Brett Synform mapped by Heather *et al.* (1995).
F. Southern Swayze		norm minerals	high strain corridor (continuation of Cadillac-Larder lake "break")
G. Western Swayze	mafic/intermediate metavolcanics	norm minerals, atypicality index	Wakami high strain zone

whereas Figures 5c and 5d were interpolated using the unaltered and altered samples, respectively. A variogram of the MgO data was constructed to firstly, test whether the data are spatially associated and secondly, to determine an appropriate *sphere of influence* around each sample point. Interpolation of the data is not justified if the variogram does not indicate that the data are spatially associated. Variogram analysis of the MgO data indicated that the data were spatially associated to a distance of approximately 3 km. This distance was used as a search radius for interpolating the data using an *inverse distance weighted* (IDW) algorithm available in the GIS.

The GIS can be used to process the data to take account of the underlying lithology on MgO concentration. This is accomplished by calculating the median MgO concentration for each lithology after performing a *point-in-polygon* operation whereby each geochemical sample point is intersected with an associated lithological map, displayed as polygons within the GIS. The following formula is then used to normalize MgO concentration for background lithology:

$$N_V = ((e / m) - 1) \times 100 \quad [3]$$

where Nv = normalized value, e = oxide or trace element concentration, and m = median value for each lithologic unit.

The median value is used in the above equation rather than the mean as it is generally less sensitive to outliers and thus is a more appropriate estimate of average background (Garrett, 1993). Values less than or equal to zero represent background values (e.g., <= than the median value for each lithological unit) while values greater than zero may represent anomalous concentrations.

Figure 5b is a contour map of MgO values after normalization for lithology using the above procedure. Note that the large east-west trending linear belt (dark zone reflecting low MgO values) defining intermediate to felsic volcanic lithologies in the central portion of the study area (see Figure 5a—"A") has been de-emphasized on the normalized image. The maps in Figure 5 display different patterns of MgO concentration and additionally, the correlation coefficients between the maps are variable (generally low) indicating they provide different visualizations for interpretation.

Geochemical data, especially trace element data, are often non-normally distributed (Garrett, 1991) requiring transformation using a log transform or Box and Cox transform (Grunsky, 1996) to produce Gaussian distributions. Normal distributions are required if further analysis involving parametric multivariate statistics are to be employed. If the data are to be used strictly for visual analysis and thresholding to determine anomalous populations, then transformation to normality is not necessary. Figure 6 is a probabilty plot of MgO concentration (wt %) for all samples. Breaks in the cumulative curves may reflect different lithologies or alteration/mineralization effects.

Many methods exist for determining thresholds for anomalous populations and include:

1. exploration knowledge (e.g., it is known that within an area of ultramafic rocks > 40 weight percent MgO is anomalous),
2. statistical methods using percentiles,
3. visual inspection of probability plots,
4. area/concentration method (Cheng *et al.*, 1994) and
5. weights of evidence (Bonham-Carter, 1994).

The *weights of evidence* method requires a priori knowledge (i.e., knowledge of existing mineral occurrences) while the other methods do not require pre-existing knowledge. The probability plots are the simplest and most effective method for determining thresholds above which the data may be considered anomalous reflecting alteration effects associated with mineralization. Breakpoints in the upper portion of the cumulative curves on probability plots, an example of which is shown on Figure 6, are used to threshold the maps shown in Figure 5. The anomalous zones determined from the thresholds have been superimposed over each map on Figure 5 (with the exception of 5f) as red, green, yellow and blue polygons. The meaning of the different colours on these maps is discussed in the following section. Any data above these breakpoints are considered anomalous. In this particular case, if the goal was to identify areas prospective for VMS exploration, then areas enriched in MgO would be of interest.

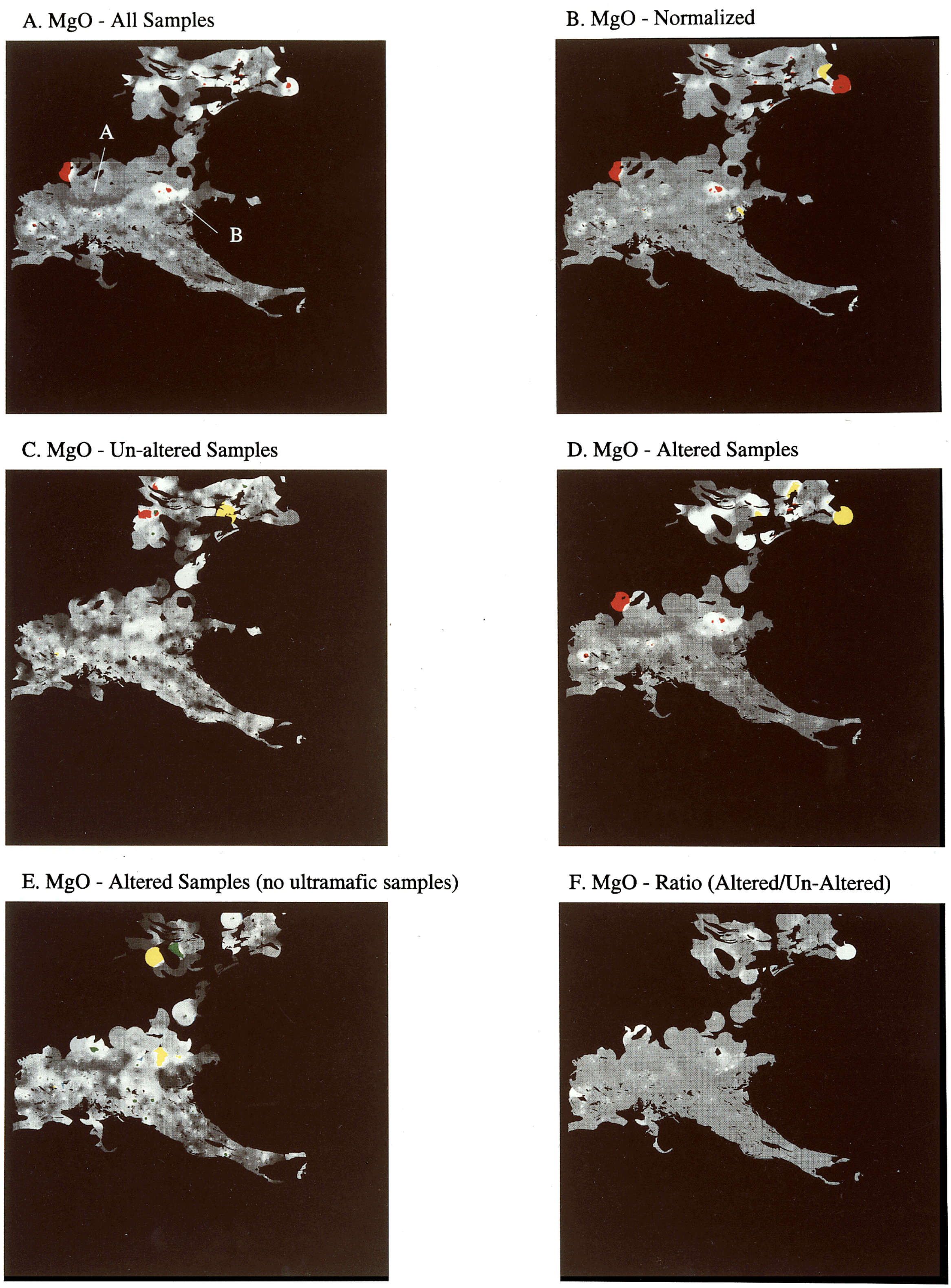

Figure 5: *Continuous surface maps of weight % MgO. Anomalous areas identified from probability plots are shown as red, green, yellow, and blue polygons. Anomalous zones shown in red are associated with geochemical samples classified as komatiites, green zones are associated with non-komatiitic samples, yellow zones are mixed, and blue have no associated points (anomaly due to interpolation of nearby points).*

Screening of Anomalies

The first step in the screening process involved deletion of anomalous zones that were due to a single sample point. This was accomplished by creating a sample density map (Harris *et al.*, 1997) and producing an uncertainty mask from this map by setting areas below a chosen density (e.g., < mean density value for the map) to zero, excluding these areas from analysis. This uncertainty mask was then used to screen out single point anomalies on the anomaly maps produced by thresholding the continuous surface maps shown in Figure 5.

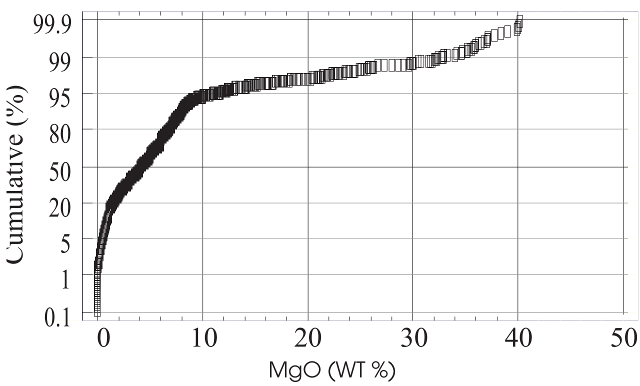

Figure 6: *Probability Plot MgO (WT %).*

The next stage in analysis involved screening the MgO anomalies, shown on Figure 5 as red, green, yellow and blue polygons, to determine whether they represent lithological variations (e.g., high MgO representing komatiites) or alteration/mineralization effects. This was accomplished in a number of different ways. Firstly, by noting the lithological unit that the anomaly fell in as well as determining the chemical classification using a Jensen cation diagram for each sample point(s) comprising the anomaly, each can be screened into different categories. If, for example, a MgO anomaly coincides with a Jensen classification of basaltic or ultramafic komatiites then there is a higher probability that the anomaly is a reflection of lithology. However, if a MgO anomaly coincides with samples classified as mafic or intermediate to felsic, then there is a higher probability that the anomaly may be due to alteration effects (e.g., MgO mobility reflecting chloritization). The MgO anomalies on Figure 5 are screened into four groups. Group 1, shown in green, represent areas that are not classified as basaltic or ultramafic komatiites and thus more likely represent alteration/mineralization effects whereas Group 2 (red areas) are classified as komatiites, and thus may simply reflect lithological variations. Group 3 (yellow) represent anomalies that are defined by multiple samples variably classified as ultramafic and other. Blue polygons are not associated with any sample point and are formed through the interpolation process of nearby sample points high in MgO. Table 3 presents a summary of whole rock samples by Jesnen classification for each anomaly shown in Figures 5a to e. The zone of high MgO concentration in the central portion of the study area (see Figure 5a—"B") coincides with a number of komatiite flows mapped by Heather *et al.* (1995).

Secondly, samples that are chemically classified as ultramafic komatiites can be excluded from the interpolation process (Figure 5e). Although this results in fewer sample points to interpolate, anomalies due to ultramafic lithologies are directly removed, as no red zones, representing komatiites, are found on this image. One has to interpret this image with caution as MgO mobility, perhaps reflecting chloritization, is a dominant chemical trend in many of the mafic and ultramafic samples in the study area as seen on Figure 2. Thus, altered ultramafic samples may still be correctly classifed and may simply involve basaltic komatiites being mis-classified as ultramafic komatiites due to MgO mobility.

Thirdly, as shown in Figure 5f, a ratio image of MgO concentration between altered and unaltered samples can be calculated. This image emphasizes the difference between altered and unaltered samples and can serve to highlight the strongest MgO anomalies.

Relationship of Known Mineral Occurrences to Oxide Anomalies

An experiment was conducted to determine which processing method resulted in the best prediction of known base metal and Au deposits. The *weights of evidence* (Agterberg, 1992; Bonham-Carter, 1994) method was used to compare the known occurrences to each of the major oxide maps processed using the above methods. The fundamental problem using the *weights of evidence* approach is to determine whether there are more deposits occurring on a map pattern (e.g., binary threshold map showing areas > 40 wt% MgO for example) than would be expected by chance. The spatial association of each binary map is assessed with respect to the location of known mineral occurrences. A pair of weights, W+ and W-, are calculated for each binary map. The weights are determined from the degree of overlap between the known occurrences and the binary pattern

Harris *et al.* (1997) provides a detailed report on this analysis. In summary it was found that generally, the oxide maps produced from the altered samples best predicted the known base metal and to a lesser extent known Au occurrences.

SUMMARY AND CONCLUSIONS

GIS is a useful tool when used in concert with other software packages (e.g., relational databases, statistical packages etc.) for compiling and manipulating and visualizing large geochemical databases. In particular, GIS facilitates the spatial analysis of the data during both the data building and evaluation stages. The results of statistical analysis such as data transforms, thresholding, chemical classifications and multivariate analysis can be displayed spatially. In addition, GIS provides many methods for visualizing, evaluating and manipulating geochemical data in both *feature space* (i.e., 2-D and 3-D scatterplots) and *geographic space* (i.e., bubble plots and RGB ternary displays).

The geochemical database has been divided into altered and unaltered populations using conventional geochemical methods. The arithmetic employed in these calculations can be performed within the GIS environment using internal databases or performed in external databases and the results imported to the GIS for display. Less traditional techniques such as the identification of unusual geochemical trends on 3-D scatterplots and the plotting of these samples in geographic space is also useful for identifying altered samples. A number of areas of intense alteration have been identified using these techniques, all of which coincide with high-strain zones. A number of these areas coincide with

Table 3: ***Summary of whole rock samples by Jensen class for each MgO anomaly map shown on Figure 5.***

	No data	CR	TR	CD	TD	CA	TA	CB	HMT	HFT	BK	PK	Total
All samples	1	2									1	30	34
Non-altered	12	2		1					7		6	6	34
Altered	1	2							3		1	32	39
Normalized	3	2				1		1	22	1	7	37	74
Altered (no BK, UM)	31	1		2		2	5	5	38	6			90

known mineralization while others are more enigmatic. Further field work is required to assess these zones.

Different methods for processing the data for mineral exploration applications have been presented. Probability plots are simple yet effective for identifying unique and possibly anomalous populations within the geochemical data. The data can be processed within the GIS to screen for lithologic and alteration effects. The MgO maps based on the altered samples and the MgO map normalized to lithology better predicted the known base metal occurrences than the raw data and the MgO map based on the unaltered samples. The maps based on the altered samples, for many of the other major oxide elements, best predicted the known mineral occurrences.

ACKNOWLEDGEMENTS

The authors would like to thank R.G. Garrett from the Geological Survey of Canada and I. Nichol from Queens University for thoughtful and constructive reviews of this manuscript. This paper is presented as GSC contribution number 1997025.

REFERENCES

Agterberg, F.P., 1992, Estimating the Probability of Occurrence of Mineral Deposits from Multiple Map Patterns *in*: In the Use of Microcomputers in Geology, Editors: Merriam, D.F. and Kurzl, H., Plenum Press, New York, pp. 73-92.

Ayer, J.A. and Theriault, R., 1993, Geology of Keith and Muskego Townships, Northern Swayze Greenstone Belt. 1192-1993 NODA Summary Report pp. 26-33.

Bonham-Carter, G.F., 1994, *Geographic Information Systems for Geoscientists: Modeling with GIS.* Pergamon (Elsevier Science Ltd.), 398 p.

Bonham-Carter, G.F., Agterberg, F., and Wright, D.F., 1988, Integration of Geological Datasets for Gold Exploration in Nova Scotia. Photogrammetric Engineering and Remote Sensing 54(11), 1585-1592.

Cheng, Q, Agterberg, F.P. and Bonham-Carter, G.F., 1994, A Spatial Analysis Method for Geochemical Anomaly Separation, Journal of Geochemical Exploration, No. 56, pp. 183-195.

Garrett, R.G., 1991, The Management, Analysis and Display of Exploration Geochemical Data, GSC Open File 2390, Geological Survey of Canada, pp. 9-1 to 9-41.

Garrett, R.G., 1993, A Cry From the Heart, Explore, Number 81, pp. 10-15.

Grunsky, E.C, Easton, R.M., Thurston, P.C., and Jensen, L.S., 1992, Characterization and Statistical Classification of Archean Volcanic Rocks of the Superior Province using Major Element Geochemistry in Geology of Ontario, Ontario Geological Survey Special Volume 4, Part 2, pp. 1347-1438.

Grunsky, E.C., 1996, Numerical Methods, Techniques and Strategies for the Evaluation and Interpretation of Geochemical Data, Short Course Notes, *in* Exploration Geochemistry in Tropical and Sub-Tropical Climates, Queens University, Kingston, Ontario, Curtin University of Technology and Cooperative Research Ctr. for Australian Mineral Exploration Technologies, 109 pp.

Harris, J.R., 1989, Data Integration for Gold Exploration in Eastern Nova Scotia Using a GIS. Proceedings of Remote Sensing for Exploration Geology, Calgary, Alberta, pp. 233-249.

Harris, J.R., Broome, J., and Heather, K.B. 1994, Swayze Greenstone Belt GIS Project. 1993-1994 NODA Summary Report p. 115-121.

Harris, J.R., Wilkinson, L., and Broome, J., 1995, Mineral Exploration Using GIS-Based Favourability Analysis, Swayze Greenstone Belt, Northern Ontario, in Proceedings of the Canadian Geomatics Conference (CD-ROM), National Defense.

Harris, J.R., Grunsky, E.C., and Wilkinson, L. 1997, Analysis of a Lithogeochemical Dataset Over the Swayze Greenstone Belt, Ontario Using a GIS, (in preparation).

Heather, K.B., Shore, T.G., and van Breeman, O., 1995, The Convoluted "Layer-cake": An Old Recipe with New Ingredients for the Swayze Greenstone Belt, Southern Superior Province, Ontario. 1994–1995 NODA Summary Report.

Jensen, L.S. 1976: A New Cation Plot for Classifying Subalkalic Volcanic Rocks. Ontario Department of Mines Misc. Paper 66, 22p.

Madiesky, H.E., and Stanley, C.R., 1993, Lithogeochemical Exploration of Metasomatic Zones Associated with Volcanic-Hosted Massive Sulphide Deposits Using Pearce Element Ratios, International Geology Review, Vol. 35, pp. 1121-1148.

Rencz, A.N., Harris, J.R., Watson, G.P., and Murphy, B., 1994, Data Integration for Mineral Exploration in the Antigonish Highlands, Nova Scotia: Application of GIS and Remote Sensing, Canadian Journal of Remote Sensing, Vol. 20, No. 3, pp. 257-267.

Rollinson, H.R. 1993: *Using Geochemical Data: Evaluation, Presentation, Interpretation.* Longman Scientific and Technical, England.

Wilkinson, L., Harris, J.R., and Grunsky, E.C., 1997, Building a Lithogeochemical Database for GIS Analysis of the Swayze Greenstone Belt; Methodology, Problems and Solutions, (in preparation).

Wright, D.F., and Bonham-Carter, G.F., 1996, VHMS Favourability Mapping with GIS-based Integration Models, Chisel Lake-Anderson Lake area. *in*: EXTECH 1: A Multidisciplinary Approach to Massive Sulphide Research in Rusty Lake-Snow Lake Greenstone Belts, Manitoba ed. G.F. Bonham-Carder, A.G. Gally, G.E.M. Hall, GSC Bulletin 426, pp. 339-376.